Transactions on Ecology and the Environment vol 17, © 1998 WIT Press, www.witpress.com, ISSN 1743-3541

Mixed Neumann/Dirichlet Boundary Conditions for Finite Element Flow Simulations in Complex Geometries

Christian Forkel, Christoph Schweim, Olaf Bergen, Volker Spork, Jürgen Köngeter

Institut für Wasserbau und Wasserwirtschaft, Aachen University of Technology, Mies-van-der-Rohe Str. 1, 52056 Aachen, Germany, E-Mail: forkel@iww.rwth-aachen.de

Abstract

The paper presents a new approach on mixed Neumann/Dirichlet boundary conditions in a finite element code for two- and three-dimensional flow simulations in irregular domains based on the Projection-2-algorithm [1]. The new approach is based on the following idea: In a first step the momentum equations are solved neglecting all Dirichlet boundary conditions on the mixed boundary nodes. Thereafter the velocities at the mixed boundaries are projected in the specified direction. In a second solution of the momentum equations, these projected velocities are now used as Dirichlet boundary conditions. Finally the projection of the calculated velocities in the divergence free subspace is done. The verification of the approach is shown as well as the problems of this method, which occurred at the practical application. The results of the developed method are compared to the results with other mixed boundary condition approaches. As a practical application, the simulation of the flow processes in a rotating annular flume is presented.

1 Introduction

The simulation of viscous flow phenomena is based on the coupled equations for mass conservation and the Navier-Stokes equations. In general it is not very efficient to solve all equations simultaneously, instead it makes sense to decouple the equations with an appropriate approach, such as it is done with the projection algorithms [1]. Then a decoupled solution of the three momentum equations and the pressure poisson equation is possible. In general the momentum equations are specified in the three cartesian coordinate directions. This causes problems, if the boundaries are not in the cartesian coordinate directions and a slip flow boundary condition or a logarithmic law of the wall shall be considered. In this case Dirichlet boundary conditions have to be defined in the normal direction ($v_i = 0$) and Neumann boundary conditions are used for the tangential directions. Solving the momentum equations in the coordinate directions then leads to mixed Neumann/Dirichlet boundary conditions, which need special treatment in the numerical approach.

2 The Mixed Boundary Condition Approach

2.1 Normal/Tangential Directions

The first problem is to define the correct normal/tangential directions at each node of a finite element boundary. Engelman et al. [2] developed a formulation for the normal and tangential direction based on the introduction of the finite element shape functions in the mass continuity equation. In three-dimensional space this leads to the following formulation of the normal direction n_j

$$n_{x_j} = \frac{1}{n_j}\int_\Omega \frac{\partial \phi_j}{\partial x} d\Omega, \quad n_{y_j} = \frac{1}{n_j}\int_\Omega \frac{\partial \phi_j}{\partial y} d\Omega, \quad n_{z_j} = \frac{1}{n_j}\int_\Omega \frac{\partial \phi_j}{\partial z} d\Omega \qquad (1)$$

$$\text{with } n_j = \sqrt{\left(\int_\Omega \frac{\partial \phi_j}{\partial x} d\Omega\right)^2 + \left(\int_\Omega \frac{\partial \phi_j}{\partial y} d\Omega\right)^2 + \left(\int_\Omega \frac{\partial \phi_j}{\partial z} d\Omega\right)^2}$$

where φ_j is the shape function at the boundary node j and Ω is the modeling domain.

If at a boundary node the type of the boundary condition is changing (for example from a slip flow boundary to an open boundary), the normal direction of this boundary node cannot be calculated by (1), but needs to be evaluated only with respect to the neighboring elements. Also it has been reported [3] that (1) does not work correctly, when quadratic shape functions are used in three-dimensional space. In this case a geometric approach for the determination of the normal directions is preferable. Then the normal direction is calculated as a weighted average of the normal directions of each neighboring boundary area:

$$n_{ij} = \frac{\sum_r \left(n_{i_r} \cdot \Gamma_r\right)}{\sum_r \Gamma_r} \quad (2)$$

where r is the number of neighboring boundary elements (at the node j) with the element boundary area Γ_r, and n_{ij} is the component of the normal vector at the node j in the cartesian direction i = x, y, z. A problem with this approach exists on curved boundaries, the calculation of the vectors n_{ij} and the element boundary areas Γ_r has yet only been investigated on non-curved grids. No matter which approach is used to determine the normal directions, the tangential directions (in 2D one tangential direction, in 3D two tangential directions) can be calculated by vector spate products.

2.2 Mixed Neumann/Dirichlet Boundary Conditions

Several approaches to solve the problem of mixed boundary conditions in non-regular domains have been reported. Hutton [4] and Hutton & Smith [5] used wall boundary elements with special shape functions, which should model the logarithmic velocity profile in these elements. But as the elements did not fulfill the mass continuity restriction and also caused stability problems, no further work with this element type was carried out. Benim & Zinser [6] and Ruprecht [7] avoid the mixed boundary conditions problem by using Dirichlet boundary conditions also for the tangential directions. The tangential velocity boundary conditions are thereby calculated from the wall stresses of the last time step together with the logarithmic law of the wall.

The new approach shown in this paper is implemented as follows in the time loop with the time step Δt:

- Solve momentum equations only with Neumann boundary conditions on the mixed boundary nodes.

  $$\frac{\partial \tilde{v}_i}{\partial t} + \tilde{v}_j \frac{\partial \tilde{v}_i}{\partial x_j} = -\frac{\partial P}{\partial x_i} + \nu \frac{\partial^2 \tilde{v}_i}{\partial x_j^{\,2}} + f_i \quad (3)$$

  with $\tilde{v}_i$: non divergence free velocity, P: kinematic pressure, ν: kinematic viscosity, f_i: body forces

- Projection of $\tilde{v}_i$ on mixed boundaries into the tangential directions of the boundary nodes

  $$v_{t,j} = \tilde{v}_i \cdot t_{i,j} \quad (4)$$

  with $v_{t,j}$: tangential velocities (j = 1 in 2D, j = 1,2 in 3D), $t_{i,j}$: tangential unity vectors (i: cartesian component of the vector)

- Projection of $v_{t,j}$ on mixed boundaries into the cartesian directions

$$\tilde{v}_{i,new} = v_{t,j} \cdot t_{i,j} \tag{5}$$

- Solve momentum equations only with Dirichlet boundary conditions $v_{i,new}$ on the mixed boundary nodes

$$\frac{\partial \tilde{v}_i}{\partial t} + \tilde{v}_j \frac{\partial \tilde{v}_i}{\partial x_j} = -\frac{\partial P}{\partial x_i} + \nu \frac{\partial^2 \tilde{v}_i}{\partial x_j^{\,2}} + f_i \tag{6}$$

- Projection of the calculated velocities $\tilde{v}_i$ on the divergence free subspace by calculating the Lagrange operator φ

$$\frac{\partial^2 \varphi}{\partial x_i} = \frac{\partial \tilde{v}_i}{\partial x_i}, \tag{7}$$

calculating the divergence free velocities

$$v_i = \tilde{v}_i - \frac{\partial \varphi}{\partial x_i}, \tag{8}$$

and actualizing the pressure

$$P_{new} = P_{old} + \frac{2\varphi}{\Delta t}, \tag{9}$$

Here the time loop continues. An iteration over the equations (3) to (9) is possible but wasn't necessary in finding a solution.

3 Verification Examples

Several different verification examples were calculated with slip flow boundary conditions in domains with edged or curved boundaries. Some of the domains are shown in Figure 1.

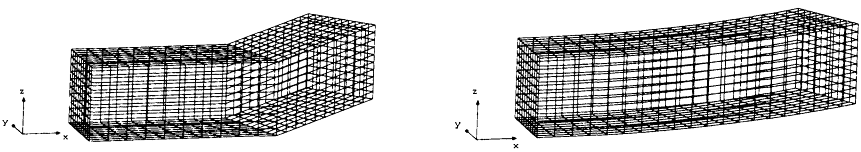

Fig. 1: Discretizations of an edged (left) and a curved (right) domain.

At the inflow on the left hand side Dirichlet boundary conditions are specified with constant velocities only in the x-direction, the outflow area is specified as an open boundary. All other boundaries have slip flow in the tangential direction and are treated as mixed Dirichlet/Neumann boundary conditions with Dirichlet boundary condition $v_n = 0$ in normal direction and Neumann boundary condition $\tau = 0$ in the tangential directions. Figure 2 shows the steady state velocity fields for the edged domain. It can be clearly seen that the velocities at the walls are always tangential to the walls. Mass control between inflow and outflow showed total mass conservation. In general all tests showed this behavior, therefore the verification was successful with one exception which is shown in Figure 3. In this test example the domain was completely rotated in space, so that no wall was tangential to any of the cartesian directions. In this test example the projection of the first time step could not find any solution that makes sense, as it is illustrated in Figure 3.

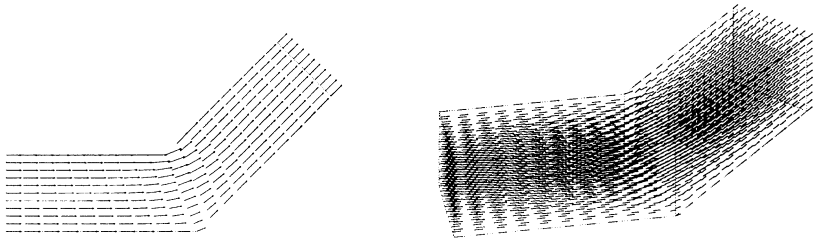

Fig. 2: Test examples velocity fields (left: horizontal cut, right: 3D-view)

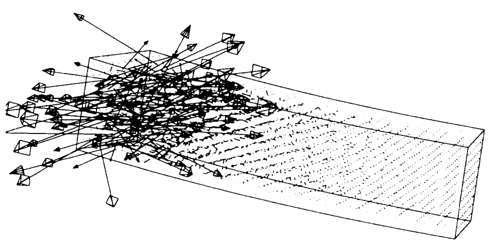

Fig. 3: 3D-view of the calculated velocity field for the curved test example rotated in space (after the projection of the first time step

No explanation for this behavior has yet been found. Especially irritating is the fact, that the same constellation gives correct results, when the mixed boundary condition wall is tangential to only one cartesian direction. From the opinion of the authors this seems to be a problem of the used solver, investigations of this problem are still going on. Anyhow, as the verification for problems with walls tangential to at least one cartesian direction was successful, an application of the algorithm to a real problem could be set up.

4 Numerical Simulation of an Annular Flume

The new mixed boundary condition approach was used in a large eddy simulation of an annular flume (Fig. 4), which is used at our institute to observe sedimentation and erosion and to determine their parameters. The bottom and the side walls of the annular flume rotate clockwise, while the top of the flume rotates counter clockwise. This leads to a flow behavior of the Couette type, so that erosion and sedimentation processes can be observed without disturbing pumping installations [10].

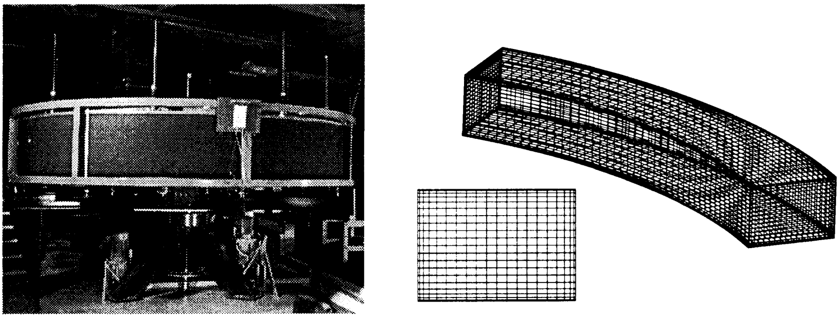

Fig. 4: Annular flume: photo and discretized area

The data of the simulated test are: Number of revolutions: bottom and side walls [in 1/min]: -2,0; Top: 3,6. Flume geometry [in m]: depth: 0,175; inner radius: 1,5; outer radius: 1,75. For the numerical simulations a large eddy model was used [9] with the large eddy constant c_S=0,1 and the filter width calculated with an adjoint volume approach which has shown to be consistent with the large eddy finite element formulation.

$$\Delta_i = \sqrt[3]{\frac{\sum_{j=1}^{m_i} V_{i_j}}{m_i}} \qquad (10)$$

V_{ij}: node related element volume, m_i: number of related element volumes.

The following boundary conditions were chosen: at the top and bottom walls we used the logarithmic law of the wall, at the side wall „slip flow“ boundary conditions were used, which led to mixed boundary conditions at these walls. The outflow boundary was simulated as an open boundary and for the inflow boundary periodic boundary conditions were chosen. To avoid backward flow through the outflow boundary, the coordinate system for the numerical simulation was of Lagrangian type and rotated together with the bottom and side walls with -2,0 revolutions per minute. Therefore also Coriolis and centrifugal forces had to be considered in the simulations. Time step length was 0,02 s.

In general the simulations showed a good agreement with the measured flow field. As one example Figure 5 shows the comparison of time averaged secondary velocities in a vertical cross section, which are extremely important for sedimentation and erosion behavior. The typical secondary eddies are calculated, but differ more or less in their extension compared to the measured values. Anyhow, these simulations gave much better results than the simulations with „no slip" boundaries at the side walls, which were carried out before.

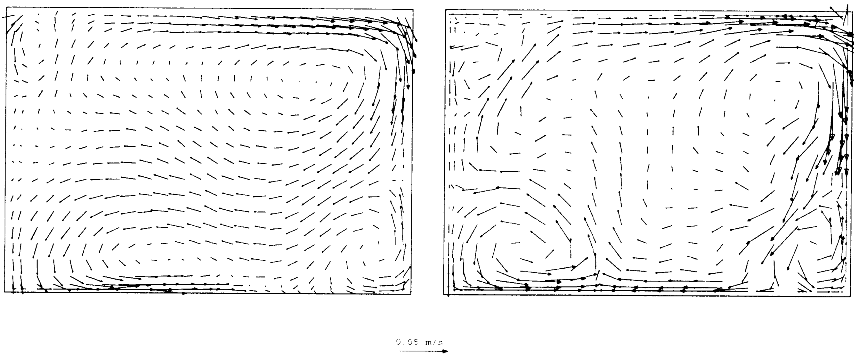

Fig. 5: Comparison of secondary velocities in a vertical cross section (inner wall on left side); left: measured values; right: simulation results

5 Conclusions and Outlook

An new approach for mixed Neumann/Dirichlet boundary conditions for finite element flow simulations with projection algorithms in irregular domains was developed and verified. The approach was used to simulate the flow in an annular flume and showed a good agreement with the measured velocity field. The approach shows some stability problems, especially if the walls have no tangential direction parallel to a cartesian direction. More investigations are necessary to overcome this problem. Also the use of logarithmic law of the wall boundary conditions as a mixed boundary condition has yet not been performed but will be investigated in near future.

Transactions on Ecology and the Environment vol 17, © 1998 WIT Press, www.witpress.com, ISSN 1743-3541

References

[1] Gresho, P.M.: „On the Theory of Semi-Implicit Projection Methods for Viscous Incompressible Flow and its Implementation via a Finite Element Method that also Introduces a Nearly-Consistent Mass Matrix, Part 1: Theory", Int. J. for Num. Meth. in Fluids, Vol. 11, pp. 587-620, 1990

[2] Engelman, M.S.; Sani, R.L.; Gresho, P.M.: „The Implementation of Normal and/ or Tangential Boundary Conditions in Finite Element Codes for Incompressible Fluid Flow", Int. J. for Num. Meth. in Fluids, Vol.2, pp. 225-238, 1982

[3] Schröder, P.-M.: „Zur numerischen Simulation turbulenter Freispiegelströmungen mit ausgeprägt dreidimensionaler Charakteristik", Mitteilungsheft Nr. 108, Institut für Wasserbau der RWTH Aachen, 1996

[4] Hutton, A.G.: „Progress in the Development of a Finite Element Wall Model for High Reynolds Number Turbulent Flow", Appl. Math. Modelling, Vol. 3, pp. 322-326, 1979

[5] Hutton, A.G.; Smith, R.M.: „On the Finite Element Simulation of Incompressible Turbulent Flow in General Two-Dimensional Geometries", Num. Meth. in Laminar and Turbulent Flow, Pineridge Press, pp. 229-242, 1981

[6] Benim, A.C.; Zinser, W.: „Investigation into the Finite Element Analysis of Confined Turbulent Flows Using a k-ε Model of Turbulence", Comp. Meth. in App. Mech. and Eng., Vo. 51, pp. 507-523, 1985

[7] Ruprecht, A.: „Finite Elemente zur Berechnung dreidimensionaler, turbulenter Strömungen in komplexen Geometrien", Institut für Hydraulische Strömungsmaschinen, Universität Stuttgart, Mitteilung Nr. 3, 1989

[8] Daniels, H.: „PASTIS-3D, Finite Element Projection Algorithm Solver for Transient Incompressible Flow Simulations", UCRL-MA-111833, Lawrence Livermore National Laboratory, CA, USA, 1992

[9] Forkel, C.: „Die Grobstuktursimulation turbulenter Strömungs- und Stoffausbreitungsprozesse in komplexen Geometrien", Mitteilungsheft Nr. 102, Institut für Wasserbau der RWTH Aachen, 1995

[10] Spork, V.: „Erosionsverhalten feiner Sedimente und ihre biogene Stabilisierung", Mitteilungsheft Nr. 114, Institut für Wasserbau der RWTH Aachen, 1997